Dalton Transactions

ROYAL SOCIETY OF CHEMISTRY

PAPER

View Article Online
View Journal | View Issue

Cite this: *Dalton Trans.*, 2025, **54**, 8241

An optical ratiometric approach using enantiopure luminescent metal complexes indicates changes in the average quadruplex DNA content as primary cells undergo multiple divisions†

Caroline Glover,‡[a,b] Simon Fairbanks,[a] Craig C. Robertson,[a] F. Richard Keene, *[c] Nicola H. Green *[b] and Jim A. Thomas *[a]

Received 19th November 2024,
Accepted 4th March 2025

DOI: 10.1039/d4dt03238a

rsc.li/dalton

The three stereoisomers of a previously reported dinuclear ruthenium(II) complex have been quantitatively separated using cation-exchange chromatography and the individual crystal structures of the racemic pair are reported. Cell-based studies on the three stereoisomers disclosed differences in the rate of uptake of the two chiral forms of the *rac* diastereoisomer with the ΛΛ-enantiomer being taken up noticeably more rapidly than the ΔΔ-form. Cell viability studies reveal that the three cations show identical cytotoxicity over 24 hours, but over more extended exposure periods, the *meso*-ΔΛ stereoisomer becomes slightly less active. More significantly, microscopy studies revealed that although both isomers display a near infra-red "light-switch" effect associated with binding to duplex DNA on binding to chromatin in live MCF7 and L5178-R cells, only the ΛΛ enantiomer displays a distinctive, blue-shifted component associated with binding to quadruplex DNA. An analysis of the ratio of "quadruplex emission" compared to "duplex emission" for the ΛΛ-enantiomer indicated that there was a decrease in the average quadruplex DNA content within live primary cells as they undergo multiple cell divisions.

Introduction

Following the report that a Pt^{II} complex intercalates into duplex DNA,[1,2] metal complexes that reversibly interact with nucleic acids have been increasingly studied. Although much initial work centred on redox-active moieties,[3–5] photo-activated systems soon attracted attention, with polypyridylruthenium(II) complexes being of particular interest.[6–12] This led to the discovery of the "DNA light-switch" $[Ru(LL)_2(dppz)]^{2+}$ (Fig. 1) (LL = 2,2′-bipyridine (bpy) or 1,10-phenanthroline (phen) and dppz = dipyridylphenazine).[13,14] The (Ru → dppz)-based ^{3}MLCT emission of this complex is suppressed in water,[15–19] but is facilitated by aprotic solvents[20–22] or through interaction with DNA[13,23,24] and other water-excluded biomolecular environments.[25,26]

Although structural studies confirmed that the prototype complex intercalates into DNA,[27–29] it is not cell permeant; however, it was found that related structures can be compartmentalised within live cells.[30,31] Over the following years, a huge number of related d^6-metal complexes that offer potential as novel cell probes,[32,33,34–41,42–49] therapeutics,[50,51,52–59,60–67] phototherapeutics[68–76] and theranostics[77,78,79–86,87] have been identified.[88–91] The interactions of such systems with higher-order DNA structures have also been studied, with quadruplex DNA being a particular focus.[92,93,94–101,102–105]

DNA quadruplexes[106–110] have been observed within cells[111–115] and assigned a range of putative biological functions from the modulation and control of gene expression[116–118] and DNA replication[119–123] to being inculcated in the aetiology of specific genetic diseases and cancers.[124–132] One facet of this research is the structure and function of telomeres, the G-rich sequences that terminate chromosomes.

Telomeres are of interest as their attrition during DNA replication defines the Hayflick limit of cell divisions before senescence.[133–136] Immortalised cells – including cancer cells

[a]*Chemistry, School of Mathematics and, Physical Sciences, Dainton Building, University of Sheffield, Sheffield, S3 7HF, UK. E-mail: james.thomas@sheffield.ac.uk*
[b]*School of Chemical, Materials and Biological Engineering, Sir Robert Hadfield Building, University of Sheffield, Sheffield, S1 3JD, UK*
[c]*Discipline of Chemistry, School of Chemistry, Physics & Earth Sciences, University of Adelaide, Adelaide, SA 5005, Australia*

†Electronic supplementary information (ESI) available: Experimental details, crystallographic tables, examples of cell viability data for the treatment of MCF7 cells, lambda stacking experiments in live MCF-7 cells, CLSM images of MCF7 cells at 670–700 nm and 630–640 nm for ΔΔ-$\mathbf{1}^{4+}$ and Λ,Λ-$\mathbf{1}^{4+}$, and the relationship between the two emission maxima for ΔΔ-$\mathbf{1}^{4+}$ and Λ,Λ-$\mathbf{1}^{4+}$ in MCF7 cells. See DOI: https://doi.org/10.1039/d4dt03238a

‡Current address: National Pathology Imaging Co-operative, St James Hospital, Leeds, LS9 7T, UK.

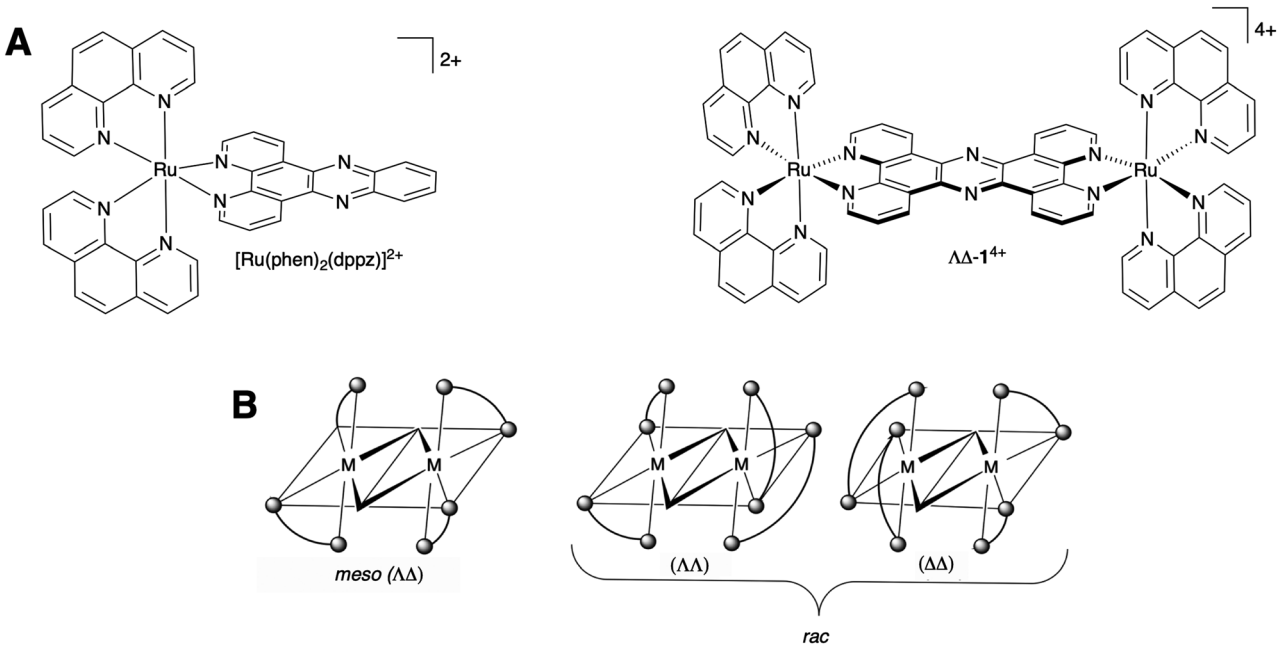

Fig. 1 (A) Structures of $[Ru(phen)_2(dppz)]^{2+}$ and ΛΔ-$\mathbf{1}^{4+}$. (B) Schematic depicting all three stereoisomers of $\mathbf{1}^{4+}$.

– maintain telomere length through the activation of telomerase or alternative telomere lengthening mechanisms.[137–141] Studies on the human telomere sequence, HTS, illustrate the structural diversity of folding in quadruplex structures *versus* duplex DNA as, depending on the experimental conditions, a variety of parallel, antiparallel and hybrid forms have been reported.[142–148]

While much work on quadruplex binding substrates has focused on therapeutics, small molecule probes for specific structures are required. The optical properties of transition metal complexes, particularly ruthenium systems, make them candidates for this role, and as part of an ongoing program to develop DNA-targeting novel luminescent probes and theranostics, the Thomas group reported the first study on light-switch-related complexes and quadruplex DNA.[94]

Although the dinuclear complex $\mathbf{1}^{4+}$ ($[\{Ru(phen)_2\}_2(\mu\text{-tpphz})]^{4+}$; tpphz = tetrapyrido[3,2-*a*:2′,3′-*c*:3″,2″-*h*:2‴,3‴-*j*]phenazine) – closely related to $[Ru(phen)_2(dppz)]^{2+}$ (Fig. 1) – is virtually non-luminescent in aqueous solution, it displays a ×50 enhancement in NIR emission (670–700 nm) when bound to duplex DNA. It also binds to anti-parallel HTS with an order of magnitude more tightly ($K_b > 10^7$ M^{-1}) and produces an intense "quadruplex light-switch" effect (luminescence enhancement: >150) that is blue-shifted by around 50 nm.[94]

Consequently, it was found that $\mathbf{1}^{4+}$ is readily taken up by live cells. Apart from its low toxicity, one striking aspect of the complex is its selectivity: co-localisation studies with commercial probes such as DAPI, SYTO-9 and PI revealed that while heterochromatin of live cells is stained, RNA is not.[45,46] These conclusions were confirmed by TEM and consequent super resolution studies.[47] Detailed studies on a variety of structures reveal that the distinctive quadruplex light-switch effect is *only* produced by quadruplexes containing diagonal loops.[149] Finally, in cell-free studies, a combination of biophysical and NMR structural data revealed that although both ΔΔ-$\mathbf{1}^{4+}$ and ΛΛ-$\mathbf{1}^{4+}$ bind to duplex DNA[150] to produce lower energy emission, showing identical binding affinities and emission enhancements, only ΛΛ-$\mathbf{1}^{4+}$ displays high affinity for HTS and the blue-shifted quadruplex light-switch signal.[151]

Herein, we report a facile and reliable procedure for the separation and isolation of ΛΛ-$\mathbf{1}^{4+}$, ΔΔ-$\mathbf{1}^{4+}$, and ΔΛ-$\mathbf{1}^{4+}$ and compare their live cell uptake, cytotoxicity, and imaging properties.

Results and discussion

Several methods have previously been used to isolate diastereomers of $\mathbf{1}^{4+}$. In previous studies, we used chirally-pure mononuclear synthons[152,153] to obtain ΛΛ-$\mathbf{1}^{4+}$ and ΔΔ-$\mathbf{1}^{4+}$. However, this method proved to be inconsistent in yields and enantiopurity, so a more reliable route to obtain the enantiomers of the racemic (*rac*) diastereomer and the *meso* diastereomer was sought. As the three diastereomers of its bpy analogue were successfully separated by cation-exchange chromatography for structural and single molecule imaging studies,[150,154] we investigated whether a similar method could be extended to separate the analogous diastereomers of $\mathbf{1}^{4+}$.

Using the cation-exchange chromatographic methods developed by the Keene group,[155–157] all three stereoisomers were separated in a two-step procedure that was slightly different to that used to separate the three stereoisomers of the close structural analogue of $\mathbf{1}^{4+}$ – $[\{Ru(bpy)_2\}_2(\mu\text{-tpphz})]^{4+}$.

Diastereomeric separation of the *rac* and *meso* forms was first accomplished by two passes down a one-metre SP Sephadex C-25 column with a 0.06 M aqueous sodium octanoate solution as the eluent. Due to the differential second-sphere association of the eluent anion with the cations, this led to the elution of discrete bands containing ΔΛ-$\mathbf{1}^{4+}$, followed by the *rac* isomer.

The chiral resolution of *rac*-$\mathbf{1}^{4+}$ was then achieved by the same technique using a higher concentration of sodium (−)-dibenzoyl-L-tartrate solution (0.15 M) as the eluent compared to that required for the resolution of *rac*-[{Ru(bpy)$_2$}$_2$(μ-tpphz)]$^{4+}$ (0.05 M).[150] Under these conditions, two discrete bands were separated in a single 1 m pass through the column (see ESI, Fig. S1†). A comparison of CD spectra with previous literature reports confirmed that ΛΛ-$\mathbf{1}^{4+}$ was eluted as the first band followed by ΔΔ-$\mathbf{1}^{4+}$ (see ESI, Fig. S2†); furthermore, the structures of the two enantiomers were confirmed by X-ray crystallography.

Good quality crystals of [ΔΔ-**1**](Cl)$_4$ were obtained by vapour diffusion of diethyl ether into nitromethane solutions, whereas [ΛΛ-**1**](PF$_6$)$_4$ was obtained by vapour diffusion of acetone into aqueous solutions of the complex – Fig. 2 and the ESI (Tables S1 and S2;† for thermal ellipsoids, see Fig. S3 and S4†).

Consistent with its chiral *P*2(1)2(1)2(1) space group, the cations in the structure of [ΔΔ-**1**](Cl)$_4$ define right-hand double helical strands (Fig. 2A). Contrastingly, in the structure of [ΛΛ-**1**](PF$_6$)$_4$, the cations are aligned within perpendicular layers (Fig. 2B). Presumably, the differences in these two structures are driven by the need to accommodate anions of different sizes within the spaces created by the cations. With the three stereoisomers of $\mathbf{1}^{4+}$ isolated, their structures confirmed, and their optical response to DNA in cell-free aqueous titrations confirmed to be consistent with our previous reports[37,98,151] (also see ESI, Fig. S5 and S6†), their uptake into MCF-7 human breast carcinoma cells individually was first investigated using confocal laser scanning microscopy (CLSM).

Time-course images of cells treated at identical concentrations, as well as the average luminescence intensity per cell in the field of view, are shown in Fig. 3. To mirror experiments we reported in our original reports using the unresolved complex,[37–39] we treated the cells with 500 μM solutions of each individual stereoisomer. Strikingly, all three stereoisomers ultimately produced the same intracellular emission intensity after ~60 minutes. Previous reports have shown that after this period, the intracellular concentration of unseparated $\mathbf{1}^{4+}$ was ~900 μM; given that each stereoisomer shows a similar emission intensity when bound to duplex DNA, these observations indicate that the final intracellular concentration of each stereoisomer was entirely comparable. Nevertheless, the rate at which this maximum is reached differs.

The stereoisomer ΛΛ-$\mathbf{1}^4$ is taken up most rapidly, with a sharp increase in emission intensity from the nucleus observed from 10 minutes onwards. Conversely, ΔΔ-$\mathbf{1}^{4+}$ shows a gradual increase in intensity over approximately 35 minutes, whereas the cellular uptake rate of the *meso* form lies between the two enantiomers. The complex is known to be taken up in an energy-dependent manner[45] and although the effect of chirality on uptake and localisation is not as pronounced as observed for some related mononuclear polypyridyl complexes,[158–160] the fact that uptake rates are dependent on the chirality of the $\mathbf{1}^{4+}$ cation offers further evidence that a specific molecular recognition process is involved.

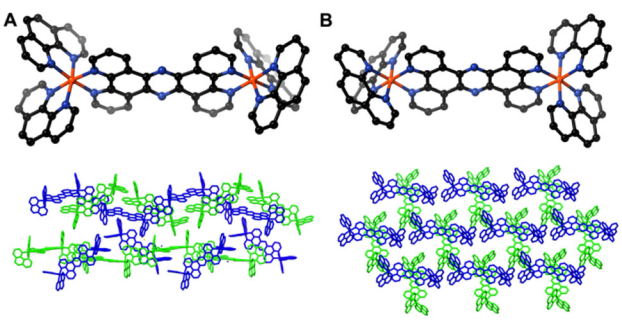

Fig. 2 Details of the crystallographic structures of [ΔΔ-**1**](Cl)$_4$ and [ΛΛ-**1**](PF$_6$)$_4$. (A) Structure of the ΔΔ-$\mathbf{1}^{4+}$ cation (top); a helical arrangement of symmetry-related cations is revealed in their packing (bottom). (B) Structure of the ΛΛ-$\mathbf{1}^{4+}$ cation (top); packing of symmetry-related cations reveals a perpendicular arrangement of layers (bottom).

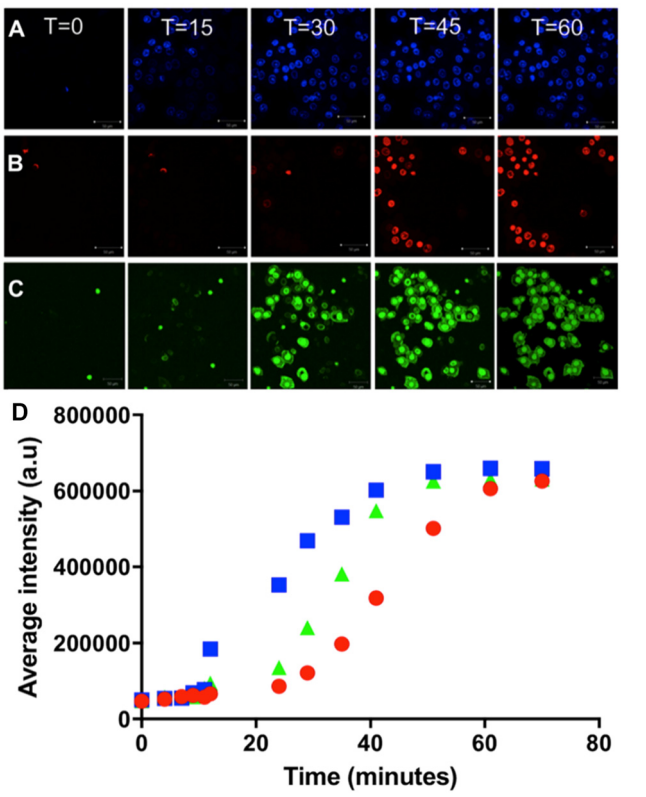

Fig. 3 MCF-7 cells treated with (A) ΛΛ-$\mathbf{1}^{4+}$, (B) ΔΔ-$\mathbf{1}^{4+}$ and (C) ΔΛ-$\mathbf{1}^{4+}$ at time points of 0, 15, 30, 45 and 60 minutes. To aid visualisation, false colour is used in these images. (D) Changes in the average luminescence intensity profiles over time (per cell in the field of view). Blue squares = ΛΛ-$\mathbf{1}^{4+}$, red circles = ΔΔ-$\mathbf{1}^{4+}$ and green triangles = ΔΛ-$\mathbf{1}^{4+}$.

In recent reports, we showed that although $\mathbf{1}^{4+}$ is not classically cytotoxic, it is antiproliferative as it blocks cytokinesis by inhibiting f-actin assembly.[65,66] As it has been demonstrated that the stereochemistry of metal complexes can have a profound effect on the cellular responses they provoke, the possibility that a particular stereoisomer of $\mathbf{1}^{4+}$ is responsible for the observed changes in cell viability was first investigated.

To test this hypothesis, the half-maximal inhibitory concentration, IC_{50}, for each stereoisomer in MCF-7 cells was determined by an MTT metabolic activity assay. To assess both cytotoxicity and antiproliferative effects, cells were treated with $\Delta\Delta$-$\mathbf{1}^{4+}$, $\Lambda\Lambda$-$\mathbf{1}^{4+}$ or $\Delta\Lambda$-$\mathbf{1}^{4+}$ for 24 and 72 hours, respectively, and compared with cisplatin under the same conditions. The results from these assays (see ESI, Fig. S7†) are summarised in Table 1.

These data show that each stereoisomer demonstrates low toxicity towards this cell line over 24 hours, which is entirely comparable to previous estimates obtained using unresolved $\mathbf{1}^{4+}$. Indeed – within the experimental error – their IC_{50} values are identical and are an order of magnitude higher than the equivalent concentration for cisplatin. As the doubling time of MCF-7 cells was determined to be ~35 hours, an extended incubation time of 72 hours allowed any effects on cell division to be examined.

Consistent with our previous report,[65] the increase in incubation time led to an appreciable decrease in IC_{50} figures for the complex. Interestingly, these figures reveal some difference between the effects of the stereoisomers on cell viability. Within error, the IC_{50} values for the enantiomeric pair $\Delta\Delta$-$\mathbf{1}^{4+}$ and $\Lambda\Lambda$-$\mathbf{1}^{4+}$ were identical and were also comparable to the IC_{50} value for cisplatin under these conditions. However, the *meso* diastereomer was less active, displaying an activity that was approximately half that of its *rac* diastereomer. These observations indicate that the interaction between $\Delta\Lambda$-$\mathbf{1}^{4+}$ and cytoskeletal elements may be slightly lower than that displayed by $\Delta\Delta$-$\mathbf{1}^{4+}$ and $\Lambda\Lambda$-$\mathbf{1}^{4+}$. Next, any differences in the imaging properties of the individual cations were investigated.

As outlined above, a combination of optical titrations, NMR structural studies, and computational methods have revealed that $\Lambda\Lambda$-$\mathbf{1}^{4+}$ is responsible for the distinctive blue-shifted "quadruplex light-switch" effect. As this effect was also seen in live cells when they were treated with an unresolved mixture of $\mathbf{1}^{4+}$, experiments to investigate whether these in-cell observations are also solely due to $\Lambda\Lambda$-$\mathbf{1}^{4+}$ were then carried out.

Initially, a procedure previously employed with unresolved $\mathbf{1}^{4+}$ and MCF-7 cells was used. Emission from the three stereoisomers was analysed in stacks at a spectral resolution of 10.8 nm, resulting in the partitioning of the duplex and quadruplex emissions into two separate "channels".

When the relationship between the two channels was analysed by plotting their intensity against each other within cell images, a plot of these data for $\Delta\Delta$-$\mathbf{1}^{4+}$ reveals a clear linear relationship between the channels, confirmed by a high R^2 value (0.96) for a fit to a straight line. As the ratio between the two wavelengths remained unchanged, the 640 nm emission was designated as merely a function of the 680 nm emission maximum. A similar analysis for $\Lambda\Lambda$-$\mathbf{1}^{4+}$ produced contrasting results as such a simple linear relationship was not observed.

The similar straight-line fit for $\Lambda\Lambda$-$\mathbf{1}^{4+}$ led to a R^2 value of ~0.75, but more distinctly, the overall average 2 : 3 ratio between the equivalent two channels for $\Lambda\Lambda$-$\mathbf{1}^{4+}$ showed that there is a considerably greater contribution from the higher energy emission compared to $\Delta\Delta$-$\mathbf{1}^{4+}$. A close comparison of individual cells revealed why this was the case: it was clear that the high-energy channel makes a non-uniform contribution to the overall emission compared to the 670–680 nm peak (see ESI, Fig. S8–10 for more details†). To further investigate this effect, a second cell line was used.

A previous study using an unseparated mixture of $\mathbf{1}^{4+}$ stereoisomers showed that the 640 nm emission was more prominent in treated L5178-R mouse lymphoma cells.[45] This was attributed to the fact that compared to MCF-7 cells – which have an average telomere length of only 2 kB – telomeres in L5178-R cells have an average length of 80 kB;[161] thus, by increasing the G-rich sequence content, the possibility of detecting quadruplex structures was increased. Similar experiments and analysis using $\Delta\Delta$-$\mathbf{1}^{4+}$ and $\Lambda\Lambda$-$\mathbf{1}^{4+}$ resulted in striking observations.

Overall rates for uptake into the murine cell line were faster than those for uptake into MCF-7 cells, with maximum emission reaching after only 40 minutes. This is probably due to the L5178-R line being grown in a suspension culture, while MCF-7 cells are adherent. Beyond this, a difference in uptake rates between the two enantiomers was also observed, with $\Lambda\Lambda$-$\mathbf{1}^{4+}$ again displaying more rapid uptake compared to $\Delta\Delta$-$\mathbf{1}^{4}$; however, a more notable difference emerges when the intracellular emissions from $\Lambda\Lambda$-$\mathbf{1}^{4+}$ and $\Delta\Delta$-$\mathbf{1}^{4+}$ are compared – Fig. 4.

The emission from $\Delta\Delta$-$\mathbf{1}^{4+}$ still shows a single emission centred at 680 nm, with the two emission channels from cells treated with $\Delta\Delta$-$\mathbf{1}^{4+}$ showing a straight-line correlation.

However, when L5178-R cells are treated with $\Lambda\Lambda$-$\mathbf{1}^{4+}$, there is a significantly greater contribution to emission from the 630–640 nm channel compared to the optical response of the same enantiomer with MCF-7 cells – Fig. 4A and B. Additionally, the higher energy emission is clearly localised within specific regions of the nucleus compared to the general chromatin staining produced by the low-energy emission – Fig. 4C. Furthermore, in cells treated with $\Lambda\Lambda$-$\mathbf{1}^{4+}$, the relationship between the two channels is nonlinear, Fig. 3D, producing a straight-line correlation of only R^2 = 0.58. As these experiments confirmed that an increase in the intensity of the

Table 1 IC_{50} values[a] against MCF7 cells for the stereoisomers of $\mathbf{1}^{4+}$

Complex	IC_{50}/μM (24 h)	IC_{50}/μM (72 h)
$\Delta\Delta$-$\mathbf{1}^{4+}$	141 ± 3	11 ± 3
$\Lambda\Lambda$-$\mathbf{1}^{4+}$	131 ± 6	7 ± 2
$\Delta\Lambda$-$\mathbf{1}^{4+}$	134 ± 4	22 ± 2
Cisplatin	13 ± 3	6 ± 2

[a] Average of three experiments.

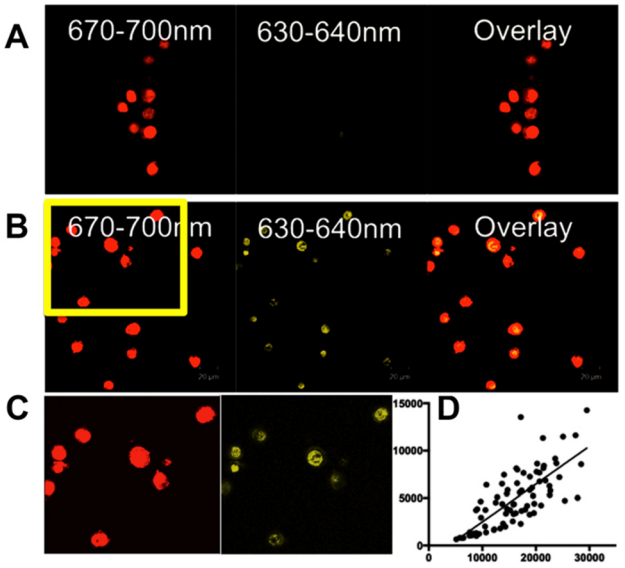

Fig. 4 L5178-R cells treated with (A) ΔΔ-$\mathbf{1}^{4+}$ and (B) ΛΛ-$\mathbf{1}^{4+}$ and (C) details of the region within the yellow box shown in (B); left: 670–700 nm, right: 630–640 nm. (D) Scatter plot for 670–700 nm emission intensity (*x*-axis) *vs.* 630–640 nm emission intensity (*y*-axis) for individual live L5178-R cells. To aid visualisation, false colour is used in these images.

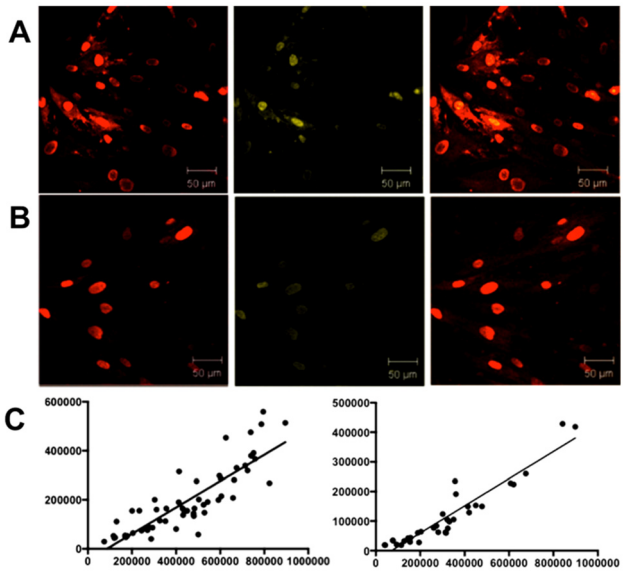

Fig. 5 HDF cells treated with ΛΛ-$\mathbf{1}^{4+}$. (A) Passage 2 cells. (B) Passage 14 cells. (C) Scatter plot for 670–700 nm emission (*x*-axis) *vs.* 630–640 nm (*y*-axis) for individual live HDF cells at passage 2 (left) and passage 14 (right).

high-energy "quadruplex channel" component in the emission of the treated L5178-R cells was observed, the use of ΛΛ-$\mathbf{1}^{4+}$ as a tool to analyse the changes in the quadruplex content in aging live primary cells was investigated.

Human dermal fibroblast (HDF) cells are known to decrease in mean telomere length by ~2 kb with each population doubling.[133,162,163] Since this shortening of G-rich telomeric DNA lowers the putative quadruplex-forming content of the live cells, we reasoned that this might be detected by changes in the high-energy emission of ΛΛ-$\mathbf{1}^{4+}$, thus we treated samples of primary HDF cells at early and late passage numbers with ΛΛ-$\mathbf{1}^{4+}$.

Before any imaging experiments were carried out, the effect of the three stereoisomers on the viability of these primary cells was first determined by an MTT metabolic activity assay employing the same conditions employed for the studies on MCF7 cells (see ESI, Fig. S11 and Table S3†). It was found that the effect of the complexes on HDF cells appeared to be slightly lowered compared to MCF7 cells, with IC_{50} values being in the range of ~150–170 μM and, again, the *meso*-form displayed the lowest cytotoxicity. The imaging properties of the complexes in HDF cells were then investigated.

Fig. 5A displays the CLSM images of HDF cells treated with ΛΛ-$\mathbf{1}^{4+}$ at passage 2, P2. As expected, the high-energy quadruplex emission channel was localised within specific areas of nuclei. A lack of uniformity with duplex emission was confirmed by a poor fit to a linear relationship between the two channels (R^2 = 0.74). In contrast, control experiments using ΔΔ-$\mathbf{1}^{4+}$ revealed a straight-line fit between the two channels (R^2 = 0.96). Untreated cells were then passaged to P14, when they were then again treated with ΔΔ-$\mathbf{1}^{4+}$ and ΛΛ-$\mathbf{1}^{4+}$. Although there was no change at all in the emission output of ΔΔ-$\mathbf{1}^{4+}$ in P14 cells compared to P2 cells, a comparison of emission from P14 cells treated with ΛΛ-$\mathbf{1}^{4+}$ showed that there was a significant decrease in the contribution from the high-energy quadruplex channel to the overall luminescence of the probe – Fig. 5B. Furthermore, the duplex and quadruplex emission channels now showed a much closer correlation to a straight line (R^2 = 0.89) – Fig. 5C.

Experimental

Separation of stereoisomers

The three stereoisomers were separated through the following procedure. The diastereomeric mixture of [**1**](PF$_6$)$_4$ (250 mg) was converted into chloride salts by metathesis with tetra-*n*-butylammonium chloride in acetone solution. The precipitated chloride salt was collected by filtration, washed with cold acetone and dried *in vacuo*. The resultant dark orange precipitate was dissolved in a minimum amount of water and introduced onto a one metre SP Sephadex C-25 column (dimensions – 26 × 100 mm). On elution with a 0.06 M sodium octanoate solution, an initial fast-moving pale-red band composed of a minor unidentified impurity was rejected. To increase the effective length of the column, once the Sephadex column had been equilibrated with the eluent, a plunger was lowered onto the surface of the support and the system was allowed to recycle with an eluent flow regulated using a peristaltic pump. After the third passage down the column, definitive separation was achieved. The *meso* (first band) and *rac* (second band) diastereomers were precipitated by the addition

of aqueous KPF_6 solution to the respective eluates. The solids were extracted with dichloromethane, and the organic extracts were dried with anhydrous Mg_2SO_4. Following filtration, the solvent was evaporated, and the residues were dried *in vacuo*. Yields: *meso*, 80 mg; *rac*, 100 mg.

Using a similar method to that described above, *rac*-[**1**][Cl]$_4$ was introduced onto a column (dimensions: 16 × 1000 mm). Upon elution with 0.15 M sodium (−)-dibenzoyl-L-tartrate solution, two distinct bands were collected and isolated as the hexafluorophosphate salts. Band 1, Δ,Δ-$\mathbf{1}^{4+}$ complex: CD λ_{max}/nm (CH_3CN) 256 ($\Delta\varepsilon$/dm^3 mol^{-1} cm^{-1}, +330.1), 269 (−471.3). Band 2, Λ,Λ-$\mathbf{1}^{4+}$ complex: CD λ_{max}/nm (CH_3CN) 256 ($\Delta\varepsilon$/dm^3 mol^{-1} cm^{-1}, −328.3), 269 (+471.7).

Conclusions

Taken together, these data and associated analysis reveal that after cells have undergone multiple passages, they display less higher-energy emission from DNA-bound ΛΛ-$\mathbf{1}^{4+}$. This suggests that the average quadruplex content of the primary cells is dependent on their replication history. One obvious contribution to this effect is the attrition of telomeres that occurs during DNA replication. Telomeres in human cells have an average length range of 10–20 kb and commonly shorten by 30–200 bases in each S-phase of the cell cycle.[162,164–167] So, although any changes in emission due to a reduction in quadruplex-folded telomeres after a single cell-doubling process will be small and are unlikely to be detected, these changes will become increasingly pronounced over a larger number of replications, which is consistent with the data presented in Fig. 5.

However, the decrease in the overall quadruplex signal may also be due to other factors linked to cellular ageing. Certainly, a recent report has demonstrated that quadruplex structures are much more abundant in stem cells and their occurrence reduces as differentiation progresses.[168] This report is one of many that indicates that dynamic quadruplex structures play a key role in the epigenetics[169,170] of even fully differentiated cells by modulating processes such as histone marking and methylation, which are also involved in the aging process. For example, it is well established that increased DNA methylation is a marker of cellular aging[171] and quadruplex forming sequences are particularly associated with "ageing clock" DNA methylation sites.[172] Yet, it has also been shown that, by inhibiting methyltransferase activity, quadruplex structures protect DNA from methylation.[173]

Finally, it seems that many processes involving dynamic quadruplex structures will be cell cycle-dependent. A case in point is the capping/uncapping of telomeres,[136,174,175] in which the folding and resolution of quadruplexes appear to play a key role. Given that not all cells in the unsynchronised populations used in this report show the same intensity and localisation of the distinctive high-energy emission, this possibility will be explored in future experiments involving synchronized cell populations.

Data availability

Supporting data have been included as part of the ESI† and crystallographic data are available from the CCDC (CCDC deposition numbers 2354069 and 2394277 for ΔΔ-$\mathbf{1}^{4+}$ and ΛΛ-$\mathbf{1}^{4+}$, respectively).

Conflicts of interest

There are no conflicts to declare.

Acknowledgements

CG is grateful to the EPSRC for the award of a Studentship. FRK and JAT acknowledge the support from the Royal Society and the Royal Society of Chemistry through their "International Exchange Award" and "Journal Grant to International Authors", respectively, for FRK's period at the University of Sheffield.

References

1 K. W. Jennette, S. J. Lippard, G. A. Vassiliades and W. R. Bauer, *Proc. Natl. Acad. Sci. U. S. A.*, 1974, **71**, 3839–3843.
2 W. I. Sundquist and S. J. Lippard, *Coord. Chem. Rev.*, 1990, **100**, 293–322.
3 D. S. Sigman, *Acc. Chem. Res.*, 1986, **19**, 180–186.
4 S. Mahadevan and M. Palaniandavar, *Inorg. Chem.*, 1998, **37**, 3927–3934.
5 B. A. Jackson and J. K. Barton, *J. Am. Chem. Soc.*, 1997, **7863**, 12986–12987.
6 J. K. Barton and E. Lolis, *J. Am. Chem. Soc.*, 1985, **107**, 708–709.
7 P. Lincoln, E. Tuite and B. Nordén, *Proc. Natl. Acad. Sci. U. S. A.*, 1992, **114**, 1454–1455.
8 K. E. Erkkila, D. T. Odom and J. K. Barton, *Chem. Rev.*, 1999, **99**, 2777–2795.
9 M. T. Carter, M. Rodriguez and A. J. Bard, *J. Am. Chem. Soc.*, 1989, **111**, 8901–8911.
10 J. M. Kelly, A. B. Tossi, D. J. Mcconnell and C. Ohuigin, *Nucleic Acids Res.*, 1985, **13**, 6017–6034.
11 F. M. O'Reilly and J. M. Kelly, *J. Phys. Chem. B*, 2000, **104**, 7206–7213.
12 F. O'Reilly, J. Kelly and A. Kirsch-De Mesmaeker, *Chem. Commun.*, 1996, 1013–1014.
13 A. E. Friedman, J. K. Barton, J. C. Chambron, J. P. Sauvage, N. J. Turro and J. K. Barton, *J. Am. Chem. Soc.*, 1990, **112**, 4960–4962.
14 C. Hiort, P. Lincoln and B. Nordén, *J. Am. Chem. Soc.*, 1993, **115**, 3448–3454.
15 E. J. C. Olson, D. Hu, A. Hörmann, A. M. Jonkman, M. R. Arkin, E. D. A. Stemp, J. K. Barton and P. F. Barbara, *J. Am. Chem. Soc.*, 1997, **119**, 11458–11467.

16 B. Önfelt, P. Lincoln, B. Nordén, J. S. Baskin and A. H. Zewail, *Proc. Natl. Acad. Sci. U. S. A.*, 2000, **97**, 5708–5713.
17 M. K. Brennaman, T. J. Meyer and J. M. Papanikolas, *J. Phys. Chem. A*, 2004, **108**, 9938–9944.
18 F. E. Poynton, J. P. Hall, P. M. Keane, C. Schwarz, I. V. Sazanovich, M. Towrie, T. Gunnlaugsson, C. J. Cardin, D. J. Cardin, S. J. Quinn, C. Long and J. M. Kelly, *Chem. Sci.*, 2016, **7**, 3075–3084.
19 A. A. Cullen, C. Long and M. T. Pryce, *J. Photochem. Photobiol., A*, 2021, **410**, 113169.
20 J. C. Chambron and J. P. Sauvage, *Chem. Phys. Lett.*, 1991, **182**, 603–607.
21 F. Biedermann, W. M. Nau and H. J. Schneider, *Angew. Chem., Int. Ed.*, 2014, **53**, 11158–11171.
22 A. W. McKinley, P. Lincoln and E. M. Tuite, *Coord. Chem. Rev.*, 2011, **255**, 2676–2692.
23 Y. Jenkins, J. K. Barton, A. E. Friedman and N. J. Turro, *Biochemistry*, 1992, **31**, 10809–10816.
24 R. M. Hartshorn and J. K. Barton, *J. Am. Chem. Soc.*, 1992, **114**, 5919–5925.
25 B. Jiang, A. Aliyan, N. P. Cook, A. Augustine, G. Bhak, R. Maldonado, A. D. Smith McWilliams, E. M. Flores, N. Mendez, M. Shahnawaz, F. J. Godoy, J. Montenegro, I. Moreno-Gonzalez and A. A. Martí, *J. Am. Chem. Soc.*, 2019, **141**, 15605–15610.
26 A. Aliyan, N. P. Cook and A. A. Martí, *Chem. Rev.*, 2019, **119**, 11819–11856.
27 H. Song, J. T. Kaiser and J. K. Barton, *Nat. Chem.*, 2012, **4**, 615–620.
28 H. Niyazi, J. P. Hall, K. O'Sullivan, G. Winter, T. Sorensen, J. M. Kelly and C. J. Cardin, *Nat. Chem.*, 2012, **4**, 621–628.
29 J. P. Hall, P. M. Keane, H. Beer, K. Buchner, G. Winter, T. L. Sorensen, D. J. Cardin, J. A. Brazier and C. J. Cardin, *Nucleic Acids Res.*, 2016, **44**, 9472–9482.
30 C. A. Puckett and J. K. Barton, *J. Am. Chem. Soc.*, 2007, **129**, 46–47.
31 C. A. Puckett and J. K. Barton, *J. Am. Chem. Soc.*, 2009, **131**, 8738–8739.
32 K. K. W. Lo, M. W. Louie and K. Y. Zhang, *Coord. Chem. Rev.*, 2010, **254**, 2603–2622.
33 J. Shum, P. K. K. Leung and K. K. W. Lo, *Inorg. Chem.*, 2019, **58**, 2231–2247.
34 L. C. C. Lee and K. K. W. Lo, *J. Am. Chem. Soc.*, 2022, **144**, 14420–14440.
35 L. C. C. Lee and K. K. W. Lo, *Chem. Rev.*, 2024, **124**, 8825–9014.
36 L. Cosgrave, M. Devocelle, R. J. Forster and T. E. Keyes, *Chem. Commun.*, 2010, **46**, 103–105.
37 A. Martin, A. Byrne, C. S. Burke, R. J. Forster and T. E. Keyes, *J. Am. Chem. Soc.*, 2014, **136**, 15300–15309.
38 F. R. Svensson, M. Matson, M. Li and P. Lincoln, *Biophys. Chem.*, 2010, **149**, 102–106.
39 F. R. Svensson, M. Abrahamsson, N. Strömberg, A. G. Ewing and P. Lincoln, *J. Phys. Chem. Lett.*, 2011, **2**, 397–401.
40 F. R. Svensson, J. Andersson, H. L. Åmand and P. Lincoln, *J. Biol. Inorg. Chem.*, 2012, **17**, 565–571.
41 W. Xu, J. Zuo, L. Wang, L. Ji and H. Chao, *Chem. Commun.*, 2014, **50**, 2123–2125.
42 K. Qiu, Y. Chen, T. W. Rees, L. Ji and H. Chao, *Coord. Chem. Rev.*, 2019, **378**, 66–86.
43 B. Z. Zhu, X. J. Chao, C. H. Huang and Y. Li, *Chem. Sci.*, 2016, **7**, 4016–4023.
44 R. Huang, M. Tang, C. H. Huang, X. J. Chao, Z. Y. Yan, J. Shao and B. Z. Zhu, *J. Phys. Chem. Lett.*, 2019, **10**, 4123–4128.
45 M. R. Gill, J. Garcia-Lara, S. J. Foster, C. Smythe, G. Battaglia and J. A. Thomas, *Nat. Chem.*, 2009, **1**, 662–667.
46 E. Baggaley, M. R. Gill, N. H. Green, D. Turton, I. V. Sazanovich, S. W. Botchway, C. Smythe, J. W. Haycock, J. A. Weinstein and J. A. Thomas, *Angew. Chem., Int. Ed.*, 2014, **53**, 3367–3371.
47 S. Sreedharan, M. R. Gill, E. Garcia, H. K. Saeed, D. Robinson, A. Byrne, A. Cadby, T. E. Keyes, C. Smythe, P. Pellett, J. Bernardino De La Serna and J. A. Thomas, *J. Am. Chem. Soc.*, 2017, **139**, 15907–15913.
48 S. Liu, H. Liang, K. Y. Zhang, Q. Zhao, X. Zhou, W. Xu and W. Huang, *Chem. Commun.*, 2015, **51**, 7943–7946.
49 A. de Almeida and R. Bonsignore, *Bioorg. Med. Chem. Lett.*, 2020, **30**, 127219.
50 H. Huang, P. Zhang, B. Yu, Y. Chen, J. Wang, L. Ji and H. Chao, *J. Med. Chem.*, 2014, **57**, 8971–8983.
51 G. Liao, X. Chen, J. Wu, C. Qian, Y. Wang, L. Ji and H. Chao, *Dalton Trans.*, 2015, **44**, 15145–15156.
52 G. Li, L. Sun, L. Ji and H. Chao, *Dalton Trans.*, 2016, **45**, 13261–13276.
53 L. Zeng, P. Gupta, Y. Chen, E. Wang, L. Ji, H. Chao and Z. S. Chen, *Chem. Soc. Rev.*, 2017, **46**, 5771–5804.
54 X. Li, A. K. Gorle, M. K. Sundaraneedi, F. R. Keene and J. G. Collins, *Coord. Chem. Rev.*, 2018, **375**, 134–147.
55 S. Thota, D. A. Rodrigues, D. C. Crans and E. J. Barreiro, *J. Med. Chem.*, 2018, **61**, 5805–5821.
56 Pragti, B. K. Kundu and S. Mukhopadhyay, *Coord. Chem. Rev.*, 2021, **448**, 214169.
57 C. Huang, T. Li, J. Liang, H. Huang, P. Zhang and S. Banerjee, *Coord. Chem. Rev.*, 2020, **408**, 213178.
58 N. A. Yusoh, H. Ahmad and M. R. Gill, *ChemMedChem*, 2020, **15**, 2121–2135.
59 N. A. Yusoh, P. R. Tiley, S. D. James, S. N. Harun, J. A. Thomas, N. Saad, L. W. Hii, S. L. Chia, M. R. Gill and H. Ahmad, *J. Med. Chem.*, 2023, **66**, 6922–6937.
60 C. E. Elgar, N. A. Yusoh, P. R. Tiley, N. Kolozsvári, L. G. Bennett, A. Gamble, E. V. Péan, M. L. Davies, C. J. Staples, H. Ahmad and M. R. Gill, *J. Am. Chem. Soc.*, 2023, **145**, 1236–1246.
61 M. Huynh, R. Vinck, B. Gibert and G. Gasser, *Adv. Mater.*, 2024, **36**, 2311437.
62 A. Notaro and G. Gasser, *Chem. Soc. Rev.*, 2017, **46**, 7317–7337.

63 A. Yadav, T. Janaratne, A. Krishnan, S. S. Singhal, S. Yadav, A. S. Dayoub, D. L. Hawkins, S. Awasthi and F. M. MacDonnell, *Mol. Cancer Ther.*, 2013, **12**, 643–653.
64 N. Alatrash, F. H. Issa, N. S. Bawazir, S. J. West, K. E. Van Manen-Brush, C. P. Shelor, A. S. Dayoub, K. A. Myers, C. Janetopoulos, E. A. Lewis and F. M. MacDonnell, *Chem. Sci.*, 2020, **11**, 264–275.
65 M. R. Gill, P. J. Jarman, V. Hearnden, S. D. Fairbanks, M. Bassetto, H. Maib, J. Palmer, K. R. Ayscough, J. A. Thomas and C. Smythe, *Angew. Chem., Int. Ed.*, 2022, **61**, e202117449.
66 A. Raza, S. A. Archer, J. A. Thomas, S. MacNeil and J. W. Haycock, *RSC Med. Chem.*, 2022, **14**, 65–73.
67 S. A. Patra, G. Sahu, S. Das and R. Dinda, *ChemMedChem*, 2023, **18**, e202300397.
68 C. Mari, V. Pierroz, A. Leonidova, S. Ferrari and G. Gasser, *Eur. J. Inorg. Chem.*, 2015, **2015**, 3879–3891.
69 F. Heinemann, J. Karges and G. Gasser, *Acc. Chem. Res.*, 2017, **50**, 2727–2736.
70 H. Huang, S. Banerjee, K. Qiu, P. Zhang, O. Blacque, T. Malcomson, M. J. Paterson, G. J. Clarkson, M. Staniforth, V. G. Stavros, G. Gasser, H. Chao and P. J. Sadler, *Nat. Chem.*, 2019, **18**, 1–15.
71 M. D. Pozza, P. Mesdom, A. Abdullrahman, T. D. Prieto Otoya, P. Arnoux, C. Frochot, G. Niogret, B. Saubaméa, P. Burckel, J. P. Hall, M. Hollenstein, C. J. Cardin and G. Gasser, *Inorg. Chem.*, 2023, **62**, 18510–18523.
72 S. A. McFarland, A. Mandel, R. Dumoulin-White and G. Gasser, *Curr. Opin. Chem. Biol.*, 2020, **56**, 23–27.
73 H. K. Saeed, P. J. Jarman, S. Archer, S. Sreedharan, I. Q. Saeed, L. K. Mckenzie, J. A. Weinstein, N. J. Buurma, C. G. W. Smythe and J. A. Thomas, *Angew. Chem., Int. Ed.*, 2017, **56**, 12628–12633.
74 S. A. Archer, A. Raza, F. Dröge, C. Robertson, A. J. Auty, D. Chekulaev, J. A. Weinstein, T. Keane, A. J. H. M. Meijer, J. W. Haycock, S. Macneil and J. A. Thomas, *Chem. Sci.*, 2019, **10**, 3502–3513.
75 A. Raza, S. A. Archer, S. D. Fairbanks, K. L. Smitten, S. W. Botchway, J. A. Thomas, S. MacNeil and J. W. Haycock, *J. Am. Chem. Soc.*, 2020, **142**, 4639–4647.
76 H. K. Saeed, S. Sreedharan, P. J. Jarman, S. A. Archer, S. D. Fairbanks, S. P. Foxon, A. J. Auty, D. Chekulaev, T. Keane, A. J. H. M. Meijer, J. A. Weinstein, C. G. W. Smythe, J. Bernardino De La Serna and J. A. Thomas, *J. Am. Chem. Soc.*, 2020, **142**, 1101–1111.
77 J. Li and T. Chen, *Coord. Chem. Rev.*, 2020, **418**, 213355.
78 C. P. Tan, Y. M. Zhong, L. N. Ji and Z. W. Mao, *Chem. Sci.*, 2021, **12**, 2357–2367.
79 S. Abdolmaleki, A. Aliabadi and S. Khaksar, *Coord. Chem. Rev.*, 2024, **501**, 215579.
80 M. R. Gill, P. J. Jarman, S. Halder, M. G. Walker, H. K. Saeed, J. A. Thomas, C. Smythe, K. Ramadan and K. A. Vallis, *Chem. Sci.*, 2018, **9**, 841–849.
81 P. J. Jarman, F. Noakes, S. Fairbanks, K. Smitten, I. K. Griffiths, H. K. Saeed, J. A. Thomas and C. Smythe, *J. Am. Chem. Soc.*, 2019, **141**, 2925–2937.
82 K. L. Smitten, H. M. Southam, J. B. de la Serna, M. R. Gill, P. J. Jarman, C. G. W. W. Smythe, R. K. Poole and J. A. Thomas, *ACS Nano*, 2019, **13**, 5133–5146.
83 K. L. Smitten, S. D. Fairbanks, C. C. Robertson, J. Bernardino De La Serna, S. J. Foster and J. A. Thomas, *Chem. Sci.*, 2020, **11**, 70–79.
84 K. L. Smitten, P. A. Scattergood, C. Kiker, J. A. Thomas and P. I. P. Elliott, *Chem. Sci.*, 2020, **11**, 8928–8935.
85 K. Smitten, H. M. Southam, S. Fairbanks, A. Graf, A. Chauvet and J. A. Thomas, *Chem. – Eur. J.*, 2023, **29**, e202203555.
86 A. M. Varney, K. L. Smitten, J. A. Thomas and S. Mclean, *ACS Pharmacol. Transl. Sci.*, 2021, **4**, 168–178.
87 M. R. Gill, M. G. Walker, S. Able, O. Tietz, A. Lakshminarayanan, R. Anderson, R. Chalk, A. H. El-Sagheer, T. Brown, J. A. Thomas and K. A. Vallis, *Chem. Sci.*, 2020, **11**, 8936–8944.
88 M. R. Gill and J. A. Thomas, *Chem. Soc. Rev.*, 2012, **41**, 3179–3192.
89 F. E. Poynton, S. A. Bright, S. Blasco, D. C. Williams, J. M. Kelly and T. Gunnlaugsson, *Chem. Soc. Rev.*, 2017, **46**, 7706–7756.
90 H. K. Saeed, S. Sreedharan and J. A. Thomas, *Chem. Commun.*, 2020, **56**, 1464–1480.
91 E. Boros, P. J. Dyson and G. Gasser, *Chem*, 2020, **6**, 41–60.
92 G. N. Grimm, A. S. Boutorine, P. Lincoln, B. Nordén and C. Hélène, *ChemBioChem*, 2002, **3**, 324–331.
93 P. Spence, J. Fielden and Z. A. E. Waller, *J. Am. Chem. Soc.*, 2020, **142**, 13856–13866.
94 C. Rajput, R. Rutkaite, L. Swanson, I. Haq and J. A. Thomas, *Chem. – Eur. J.*, 2006, **12**, 4611–4619.
95 S. N. Georgiades, N. H. Abd Karim, K. Suntharalingam and R. Vilar, *Angew. Chem., Int. Ed.*, 2010, **49**, 4020–4034.
96 L. Xu, D. Zhang, J. Huang, M. Deng, M. Zhang and X. Zhou, *Chem. Commun.*, 2010, **46**, 743–745.
97 L. Xu, X. Chen, J. Wu, J. Wang, L. Ji and H. Chao, *Chem. – Eur. J.*, 2014, **21**, 4008–4020.
98 E. Wachter, D. Moyá, S. Parkin and E. C. Glazer, *Chem. – Eur. J.*, 2016, **22**, 550–559.
99 G. Piraux, L. Bar, M. Abraham, T. Lavergne, H. Jamet, J. Dejeu, L. Marcélis, E. Defrancq and B. Elias, *Chem. – Eur. J.*, 2017, **23**, 11872–11880.
100 J. Weynand, A. Diman, M. Abraham, L. Marcélis, H. Jamet, A. Decottignies, J. Dejeu, E. Defrancq and B. Elias, *Chem. – Eur. J.*, 2018, **24**, 19216–19227.
101 K. McQuaid, H. Abell, S. P. Gurung, D. R. Allan, G. Winter, T. Sorensen, D. J. Cardin, J. A. Brazier, C. J. Cardin and J. P. Hall, *Angew. Chem., Int. Ed.*, 2019, **58**, 9881–9885.
102 M. Gillard, G. Piraux, M. Daenen, M. Abraham, L. Troian-Gautier, L. Bar, H. Bonnet, F. Loiseau, H. Jamet, J. Dejeu, E. Defrancq and B. Elias, *Chem. – Eur. J.*, 2022, **28**, e20220225.
103 S. J. Devereux, F. E. Poynton, F. R. Baptista, T. Gunnlaugsson, C. J. Cardin, I. V. Sazanovich, M. Towrie, J. M. Kelly and S. J. Quinn, *Chem. – Eur. J.*, 2020, **26**, 17103–17109.

104 K. Xiong, C. Ouyang, J. Liu, J. Karges, X. Lin, X. Chen, Y. Chen, J. Wan, L. Ji and H. Chao, *Angew. Chem., Int. Ed.*, 2022, **61**, e202204866.
105 M. Stitch, D. Avagliano, D. Graczyk, I. P. Clark, L. González, M. Towrie and S. J. Quinn, *J. Am. Chem. Soc.*, 2023, **145**, 21344–21360.
106 S. Burge, G. N. Parkinson, P. Hazel, A. K. Todd and S. Neidle, *Nucleic Acids Res.*, 2006, **34**, 5402–5415.
107 P. Hazel, G. N. Parkinson and S. Neidle, *J. Am. Chem. Soc.*, 2006, **128**, 5480–5487.
108 R. D. Gray, J. O. Trent and J. B. Chaires, *J. Mol. Biol.*, 2014, **426**, 1629–1650.
109 J. Spiegel, S. Adhikari and S. Balasubramanian, *Trends Chem.*, 2020, **2**, 123–136.
110 D. Varshney, J. Spiegel, K. Zyner, D. Tannahill and S. Balasubramanian, *Nat. Rev. Mol. Cell Biol.*, 2020, **21**, 459–474.
111 E. Y. N. Lam, D. Beraldi, D. Tannahill and S. Balasubramanian, *Nat. Commun.*, 2013, **4**, 1796.
112 J. J. King, K. L. Irving, C. W. Evans, R. V. Chikhale, R. Becker, C. J. Morris, C. D. Peña Martinez, P. Schofield, D. Christ, L. H. Hurley, Z. A. E. Waller, K. S. Iyer and N. M. Smith, *J. Am. Chem. Soc.*, 2020, **142**, 20600–20604.
113 W. C. Huang, T. Y. Tseng, Y. T. Chen, C. C. Chang, Z. F. Wang, C. L. Wang, T. N. Hsu, P. T. Li, C. T. Chen, J. J. Lin, P. J. Lou and T. C. Chang, *Nucleic Acids Res.*, 2015, **43**, 10102–10113.
114 M. Di Antonio, A. Ponjavic, A. Radzevičius, R. T. Ranasinghe, M. Catalano, X. Zhang, J. Shen, L. M. Needham, S. F. Lee, D. Klenerman and S. Balasubramanian, *Nat. Chem.*, 2020, **12**, 832–837.
115 P. A. Summers, B. W. Lewis, J. Gonzalez-Garcia, R. M. Porreca, A. H. M. Lim, P. Cadinu, N. Martin-Pintado, D. J. Mann, J. B. Edel, J. B. Vannier, M. K. Kuimova and R. Vilar, *Nat. Commun.*, 2021, **12**, 162.
116 A. Siddiqui-Jain, C. L. Grand, D. J. Bearss and L. H. Hurley, *Proc. Natl. Acad. Sci. U. S. A.*, 2002, **99**, 11593–11598.
117 S. Rankin, A. P. Reszka, J. Huppert, M. Zloh, G. N. Parkinson, A. K. Todd, S. Ladame, S. Balasubramanian and S. Neidle, *J. Am. Chem. Soc.*, 2005, **127**, 10584–10589.
118 T. Tian, Y. Q. Chen, S. R. Wang and X. Zhou, *Chem*, 2018, **4**, 1314–1344.
119 K. Paeschke, J. A. Capra and V. A. Zakian, *Cell*, 2011, **145**, 678–691.
120 D. Rhodes and H. J. Lipps, *Nucleic Acids Res.*, 2015, **43**, 8627–8637.
121 A. L. Valton and M. N. Prioleau, *Trends Genet.*, 2016, **32**, 697–706.
122 L. K. Lerner and J. E. Sale, *Genes*, 2019, **10**, 95.
123 P. Prorok, M. Artufel, A. Aze, P. Coulombe, I. Peiffer, L. Lacroix, A. Guédin, J. L. Mergny, J. Damaschke, A. Schepers, B. Ballester and M. Méchali, *Nat. Commun.*, 2019, **10**, 1–16.
124 R. Simone, P. Fratta, S. Neidle, G. N. Parkinson and A. M. Isaacs, *FEBS Lett.*, 2015, **589**, 1653–1668.
125 N. Maizels, *EMBO Rep.*, 2015, **16**, 910–922.
126 Y. V. Suseela, N. Narayanaswamy, S. Pratihar and T. Govindaraju, *Chem. Soc. Rev.*, 2018, **47**, 1098–1131.
127 Y. Wang, J. Yang, A. T. Wild, W. H. Wu, R. Shah, C. Danussi, G. J. Riggins, K. Kannan, E. P. Sulman, T. A. Chan and J. T. Huse, *Nat. Commun.*, 2019, **10**, 1–14.
128 D. Liano, S. Chowdhury and M. Di Antonio, *J. Am. Chem. Soc.*, 2021, **143**, 20988–21002.
129 S. Balasubramanian, L. H. Hurley and S. Neidle, *Nat. Rev. Drug Discovery*, 2011, **10**, 261–275.
130 S. Neidle, *Nat. Rev. Chem.*, 2017, **1**, 1–10.
131 R. Hänsel-Hertsch, A. Simeone, A. Shea, W. W. I. Hui, K. G. Zyner, G. Marsico, O. M. Rueda, A. Bruna, A. Martin, X. Zhang, S. Adhikari, D. Tannahill, C. Caldas and S. Balasubramanian, *Nat. Genet.*, 2020, **52**, 878–883.
132 R. C. Monsen, *Front. Chem.*, 2023, **11**, 1211512.
133 C. B. Harley, A. B. Futcher and C. W. Greider, *Nature*, 1990, **345**, 458–460.
134 T. De Lange, *Nat. Rev. Mol. Cell Biol.*, 2004, **5**, 323–329.
135 T. De Lange, *Science*, 2009, **326**, 948–952.
136 J. W. Shay and W. E. Wright, *Nat. Rev. Genet.*, 2019, **20**, 299–309.
137 S. E. Artandi and R. A. DePinho, *Carcinogenesis*, 2009, **31**, 9–18.
138 P. J. Campbell, *Cell*, 2012, **148**, 633–635.
139 J. Maciejowski and T. De Lange, *Nat. Rev. Mol. Cell Biol.*, 2017, **18**, 175–186.
140 A. J. Cesare and R. R. Reddel, *Nat. Rev. Genet.*, 2010, **11**, 319–330.
141 R. L. Flynn, K. E. Cox, M. Jeitany, H. Wakimoto, A. R. Bryll, N. J. Ganem, F. Bersani, J. R. Pineda, M. L. Suvà, C. H. Benes, D. A. Haber, F. D. Boussin and L. Zou, *Science*, 2015, **347**, 273–277.
142 Y. Wang and D. J. Patel, *Structure*, 1993, **1**, 263–282.
143 G. N. Parkinson, M. P. H. Lee and S. Neidle, *Nature*, 2002, **417**, 876–880.
144 K. N. Luu, A. T. Phan, V. Kuryavyi, L. Lacroix and D. J. Patel, *J. Am. Chem. Soc.*, 2006, **128**, 9963–9970.
145 A. T. Phan, V. Kuryavyi, K. N. Luu and D. J. Patel, *Nucleic Acids Res.*, 2007, **35**, 6517–6525.
146 K. W. Lim, P. Alberti, A. Guédin, L. Lacroix, J. F. Riou, N. J. Royle, J. L. Mergny and A. T. Phan, *Nucleic Acids Res.*, 2009, **37**, 6239–6248.
147 B. Heddi and A. T. Phan, *J. Am. Chem. Soc.*, 2011, **133**, 9824–9833.
148 R. C. Monsen, S. Chakravarthy, W. L. Dean, J. B. Chaires and J. O. Trent, *Nucleic Acids Res.*, 2021, **49**, 1749–1768.
149 T. Wilson, M. P. Williamson and J. A. Thomas, *Org. Biomol. Chem.*, 2010, **8**, 2617–2621.
150 S. D. Fairbanks, C. C. Robertson, F. R. Keene, J. A. Thomas and M. P. Williamson, *J. Am. Chem. Soc.*, 2019, **141**, 4644–4652.
151 T. Wilson, P. J. Costa, V. V. Félix, M. P. Williamson and J. A. Thomas, *J. Med. Chem.*, 2013, **56**, 8674–8683.
152 B. Bosnich and F. P. Dwyer, *Aust. J. Chem.*, 1966, **19**, 2229–2233.

153 X. Hua and A. von Zelewsky, *Inorg. Chem.*, 1995, **34**, 5791–5797.
154 M. D. Newton, S. D. Fairbanks, J. A. Thomas and D. S. Rueda, *Angew. Chem., Int. Ed.*, 2021, **60**, 20952–20959.
155 N. C. Fletcher, P. C. Junk, D. A. Reitsma and F. R. Keene, *J. Chem. Soc., Dalton Trans.*, 1998, **2**, 133–138.
156 F. Richard Keene, *Chem. Soc. Rev.*, 1998, **27**, 185–193.
157 N. C. Fletcher and F. R. Keene, *J. Chem. Soc., Dalton Trans.*, 1999, 683–689.
158 Z. P. Zeng, Q. Wu, F. Y. Sun, K. Di Zheng and W. J. Mei, *Inorg. Chem.*, 2016, **55**, 5710–5718.
159 R. Huang, F. P. Feng, C. H. Huang, L. Mao, M. Tang, Z. Y. Yan, B. Shao, L. Qin, T. Xu, Y. H. Xue and B. Z. Zhu, *ACS Appl. Mater. Interfaces*, 2020, **12**, 3465–3473.
160 R. Huang, C. H. Huang, J. Chen, Z. Y. Yan, M. Tang, J. Shao, K. Cai and B. Z. Zhu, *Nucleic Acids Res.*, 2023, **51**, 11981–11998.
161 A. Canela, E. Vera, P. Klatt and M. A. Blasco, *Proc. Natl. Acad. Sci. U. S. A.*, 2007, **104**, 5300–5305.
162 R. C. Allsopp, H. Vaziri, C. Patterson, S. Goldstein, E. V. Younglai, A. B. Futcher, C. W. Greider and C. B. Harley, *Proc. Natl. Acad. Sci. U. S. A.*, 1992, **89**, 10114–10118.
163 U. M. Martens, E. A. Chavez, S. S. S. Poon, C. Schmoor and P. M. Lansdorp, *Exp. Cell Res.*, 2000, **256**, 291–299.
164 N. D. Hastie, M. Dempster, M. G. Dunlop, A. M. Thompson, D. K. Green and R. C. Allshire, *Nature*, 1990, **346**, 866–868.
165 R. C. Allsopp, E. Chang, M. Kashefi-Aazam, E. I. Rogaev, M. A. Piatyszek, J. W. Shay and C. B. Harley, *Exp. Cell Res.*, 1995, **220**, 194–200.
166 G. Aubert, M. Hills and P. M. Lansdorp, *Mutat. Res., Fundam. Mol. Mech. Mutagen.*, 2012, **730**, 59–67.
167 J. Aguado, F. d'Adda di Fagagna and E. Wolvetang, *Ageing Res. Rev.*, 2020, **62**, 101115.
168 K. G. Zyner, A. Simeone, S. M. Flynn, C. Doyle, G. Marsico, S. Adhikari, G. Portella, D. Tannahill and S. Balasubramanian, *Nat. Commun.*, 2022, **13**, 1–17.
169 A. K. Mukherjee, S. Sharma and S. Chowdhury, *Trends Genet.*, 2019, **35**, 129–144.
170 A. Malousi, A. Z. Andreou, E. Georgiou, G. Tzimagiorgis, L. Kovatsi and S. Kouidou, *Epigenetics*, 2018, **13**, 808–821.
171 K. Seale, S. Horvath, A. Teschendorff, N. Eynon and S. Voisin, *Nat. Rev. Genet.*, 2022, **23**, 585–605.
172 J. Rauchhaus, J. Robinson, L. Monti and M. Di Antonio, *Genes*, 2022, **13**, 1665.
173 S. Q. Mao, A. T. Ghanbarian, J. Spiegel, S. Martínez Cuesta, D. Beraldi, M. Di Antonio, G. Marsico, R. Hänsel-Hertsch, D. Tannahill and S. Balasubramanian, *Nat. Struct. Mol. Biol.*, 2018, **25**, 951–957.
174 M. L. Bochman, K. Paeschke and V. A. Zakian, *Nat. Rev. Genet.*, 2012, **13**, 770–780.
175 J. S. Smith, Q. Chen, L. A. Yatsunyk, J. M. Nicoludis, M. S. Garcia, R. Kranaster, S. Balasubramanian, D. Monchaud, M. P. Teulade-Fichou, L. Abramowitz, D. C. Schultz and F. B. Johnson, *Nat. Struct. Mol. Biol.*, 2011, **18**, 478–486.